# Optimized Detection of Hypoglycemic Glucose Ranges in Human Serum by Raman Spectroscopy with 532 nm Laser Excitation

Ata Golparvar[1,*][a], Assim Boukhayma[1,2], Christian Enz[1] and Sandro Carrara[1]

[1]*Integrated Circuit Laboratory, École Polytechnique Fédérale de Lausanne (EPFL), CH-2002 Neuchâtel, Switzerland*
[2]*Senbiosys SA, CH-2002 Neuchâtel, Switzerland*

Keywords: Blood Plasma, Continuous Monitoring, Glucometer, Glucose Monitoring, Human Serum Analysis, Non-invasive, Raman Effect, Vibrational Spectroscopy.

Abstract: Raman scattering-based biomedical detection has usually been proposed with near-infrared laser sources. However, a low-cost CMOS imager's quantum efficiency is optimum around green wavelength, and their sensitivity substantially decreases in near-infrared wavelengths. Additionally, since Raman scattering intensity is proportional to $\lambda^{-4}$, where $\lambda$ is the laser wavelength, the increase of wavelength directly results in less sensitive measurement. These facts contribute to limiting the transfer of detection methodologies based on Raman spectroscopy to portable and low-cost point-of-care medical devices. Therefore, here we propose 532 nm green laser-induced Raman spectroscopy for low human serum glucose level detection. However, in 532 nm Raman spectroscopy of carotenoid containing biological systems, such as human serum, resonance Raman occurs, and total carotenoids resonance bands dominate the spectra. To demonstrate serum glucose detection on concentration levels typical in severe hypoglycemic ranges, this study optimizes laser focal depth, laser excitation duration, and laser power to extend the sensitivity by exploiting the glucose Raman shift peak at $1125 \pm 7.5$ cm$^{-1}$. By applying experimentally tuned parameters, our findings suggest sensitive detection of serum glucose in the range of 0–10 mmol/l with 1.2 mmol/l theoretical limit of detection (LOD) by using spontaneous (non-enhanced) Raman spectroscopy.

## 1 INTRODUCTION

The number of diabetes patients has increased significantly (B. Zhou et al., 2016), and "diabetes management" has been a severe public health burden expected to double by 2030 compared to 2015 statistics (Bommer et al., 2018). Diabetes mellitus is a chronic disorder that impairs glucose homeostasis (Chege, Birech, Mwangi, & Bukachi, 2019). To survive, diabetic patients must prevent its severe secondary complications by frequent monitoring to keep the glucose level under control through adequate insulin injection (Zimmet, Alberti, & Shaw, 2001). To monitor blood glucose levels reliably, patients depend on frequent finger-prick tests to draw out capillary blood, which is painful and inconvenient with the potential cross-contamination risk when the

lancet is reused or not properly sterilized (Ju et al., 2020). Additionally, finger pricking is closely related to diabetes burnout—a state of detachment from diabetic care (Zimmet et al., 2001), directly related to diabetes-induced morbidity and mortality (Abdoli, Hessler, Vora, Smither, & Stuckey, 2020). Therefore, optical detection techniques have been proposed for non-invasive glucose monitoring and reviewed extensively (Smith, 2015). Among them, Raman spectroscopy holds great potential thanks to its high specificity due to the unique chemical "fingerprint" signature of inelastic scattering of photons from each specific analyte (Singh, Goh, Canzoneri, & Ram, 2015). Furthermore, it promises an excellent alternative for rapid, label-free, and non-invasive detection in biomedical applications (Lawson, Barry, Williams, & Edwards, 1997), such as continuous glucose concentration monitoring in human tissue

---

[a] https://orcid.org/0000-0002-1107-6380
* Corresponding author

due to its water-insensitive probing (Gulyamov et al., 2021; Kang et al., 2020). Raman effect occurs when a molecule interacts with an incident photon and is driven to a virtual state. With a slim chance the molecule relaxes to a vibrational state other than the original ground state, due to the quantum energy exchange with the incident photon and the molecule's vibrational modes, dictated by their unique energy difference (Krishnan & Shankar, 1981).

Although spontaneous Raman offers a small scattering cross-section, it is still more robust for glucose level estimation than other absorption-based vibrational spectroscopy techniques due to the water's inadequate scattering response but high absorbance signature (Li, Deen, Kumar, & Selvaganapathy, 2014). However, since Raman scattering is a weak process, its application to low glucose concentration (i.e., below 5 mmol/l) detection is problematic and to perform such measurements, often long acquisition time or high laser powers are needed. On the other hand, to enhance the Raman effect, which may indeed lower the measurement's required acquisition time and laser power, techniques such as plasmonic surface enhancement, resonance Raman exploitation, and non-linear coherent process have been suggested over the years (Kiefer, 2007; Li et al., 2014). Even though surface enhancement is most effective with metallic nanoparticle surfaces, the subcutaneous injection of metallic materials can produce toxicity (Asharani, Wu, Gong, & Valiyaveettil, 2008) and require surgical implant placement (Stuart et al., 2006), which removes the technique from the non-invasive application. On the other hand, resonant Raman spectroscopy usually requires a low wavelength in ultra-violet ranges for the excitation laser. However, such low wavelengths hold risks of photochemical damage to the tissue being investigated (Mhlanga, Tetyana, Nyembe, & Sikhwivhilu, 2021), and thus this hinders the technique from the non-invasive application as well. Nonetheless, coherent Raman scattering might be favored in the light of newly emerged technologies on the side of cheap and low noise CMOS image sensors (Boukhayma, 2018).

Even though spontaneous Raman has not been primarily considered for low glucose level detection, mainly due to the expressed reasons, we propose spontaneous Raman spectroscopy to address the need to improve the sensitivity toward low concentration range. In fact, in the absence of any Raman enhancement, the excitation laser wavelength selection is perhaps the most critical design parameter. In particular, Raman scattering intensity is proportional to $\lambda^{-4}$, where $\lambda$ is the laser wavelength

(Šugar & Bouř, 2016). Due to that, 532 nm green laser is theoretically 4.7 times more efficient than 785 nm near-infrared laser and theoretically 16 times better efficiency than a 1064 nm infrared laser source. Of course, blue or violate lasers are even better than green lasers, but they are still costly (Greer, Petrov, & Yakovlev, 2013), and the quantum efficiency of low-cost silicon-CMOS imagers decays rapidly below the green wavelengths (Boukhayma, Peizerat, & Enz, 2016).

Recent investigations have shown that human serum does not produce strong autofluorescence to completely mask the Raman spectra in the visible range with 532 nm green lasers and can be filtered out using the available chemometric tools, different from what is observed already with 660 nm red laser (Medipally et al., 2017). Thus, acquiring 532 nm is highly advantageous for improving the intensity of the Raman scattering measurement. Furthermore, a 532 nm laser choice is optimum due to the highest quantum efficiency of the CMOS imagers in the green wavelengths (Wróbel, 2016), and therefore a much better solution from the perspective of portable Raman devices for glucose sensing. To succeed on that, we need to consider the interference by carotenoids, which resonance Raman shift is at 1153 $cm^{-1}$, extremely close to that of the glucose that shows its characteristic band around 1125 $cm^{-1}$. Therefore, this study deeply investigated the possible optimizations on laser focal depth, laser excitation duration, and laser power to optimize especially for serum glucose levels in severe hypoglycemic ranges by exploiting the Raman shift peak of $1125 \pm 7.5$ $cm^{-1}$ with spontaneous and non-enhanced Raman spectroscopy.

## 2 METHODOLOGY

### 2.1 Sample Preparation

D-(+)-glucose powder ($C_6H_{12}O_6$, purity $\geq 99.5\%$) and human serum solution (male AB plasma, sterile-filtered, stored in -20 °C) were purchased from Sigma-Aldrich (MilliporeSigma, MO, USA). Reagents were analytical grade and were used as received. Glucose stock solutions with concentrations of 200 mmol/l and 100 mmol/l (25 ml each) were prepared to dilute and spike the serum's glucose concentration to various amounts to explore the dynamic range and sensitivity of the measurements. The powder was carefully measured with a highly precise scale and wholly dissolved in nanopure water. The concentrations were selected to cover a wide

range of human blood serum glucose levels to simulate normal and unstable conditions (i.e., hypoglycemia or hyperglycemia) as well as to more extensive concentration ranges (up 100 mmol/l) to the straightforward demonstration of the detection principle. Hypoglycemia was defined as a blood glucose level smaller than 3.9 mmol/l (70 mg/dl), whereas hyperglycemia was identified when it is above 10 mmol/l (180 mg/dl) (Brinati et al., 2021). Therefore, glucose stock solutions were diluted to prepare 1.5 mL spiked serum solutions (0.75 mL glucose mixed with 0.75 mL serum) with overall glucose concentrations of 1–10 mmol/l (18–180 mg/dl) and 20-100 mmol/l (360–1800 mg/dl) with intervals of 1 mmol/l and 20 mmol/l, respectively, and were refrigerated overnight. Each sample was first stirred during the measurement session, and then a 20-µl droplet of each liquid was placed into a concave glass microscope slides with well depths of ~ 800 µm (Electron Microscopy Sciences PA, USA) using a micropipette (Gilson International, France).

## 2.2 Data Acquisition and Optimization

In the backscattered configuration, the Raman spectra of human serum solutions were obtained with confocal micro-Raman microscopy (LabRAM HR, Horiba, Japan), exploiting the spectral region of 200–1900 $cm^{-1}$ using a liquid-nitrogen-cooled CCD camera. The excitation source was a 532 nm single-frequency green laser (Cobolt 05, Hubner Photonics, Germany). Different laser powers varying from 0.4 mW to 400 mW and different acquisition durations changing from 10 s to 180 s were tested to optimize the best sensitivity within the fastest acquisition time for low glucose level detection in human serum. To further optimize the Raman scattering intensity, the filtered beam was focused to the surface as well as to the 200 µm, 400 µm, and 600 µm below the surface of the droplet using a long working distance ×50 objective lens with NA of 0.50 (LMPLFLN, Olympus Corporation, Japan). The beam quality was M2 < 1.1, beam diameter (1/e²) at the objective input was 2 mm, and objective lens focal length was 180 mm. The spectrometer was adjusted to groove density of 600 g/mm, the slit size of 100 µm, and the confocal hole size of 200 µm. Higher grating values increase the spectral resolution while decreasing spectral coverage, and larger slit and confocal hole size increase the intensity at the cost of spectral resolution (F Adar, Lee, Mamedov, & Whitley, 2010; Tuschel, 2020). The spectral resolution of this univariate analysis study is critical since the targeted glucose 1125 $cm^{-1}$ band is essentially a single shoulder peak.

Therefore, the spectral resolution should be high enough to identify the main Raman peak of interest by the nearby prominent carotenoids resonance 1153 $cm^{-1}$ peak. At the same time, Raman scattering intensity is crucial to obtain high sensitivity in low concentration levels. Therefore, we decided to select a configuration to maintain a fair balance between spectral resolution and Raman intensity. Calibration of the spectrometer was carried with 520 $cm^{-1}$ characteristic peak of silicon. Three consecutive spectra were obtained using different droplets to compute the measurement error, and no photodamage or photo-degradation was observed. Throughout the experiments, the room was dark, and 24°C was maintained.

All data processing was performed with Origin (OriginLab Corporation, MA, USA). For each spectrum, the autofluorescence induced baseline was subtracted using the asymmetric least-square fit (asymmetric factor 0.001, threshold 0.02, smoothing factor 5, and iteration 10), then the Savitzky-Golay filter (polynomial order 3, window length 13) was applied to smooth the spectrum further (Zimmet et al., 2001). The absolute area under the Raman shift peak of 1125 ± 7.5 $cm^{-1}$ was integrated to perform the univariate analysis and predict the serum glucose level, and linear regression fit was used to draw the calibration curve and calculate the measurement sensitivity.

## 3 RESULTS AND DISCUSSION

Figure 1a illustrates the processed Raman scattering spectra of human serum spiked with glucose, pure aqueous glucose, and pure serum solutions. The intensities of Raman scattering bands are directly proportional to the concentration of solution analytes, and for aqueous glucose, this is typically observed in multiple peaks around 437, 518, 1060, 1125, and 1365 $cm^{-1}$ bands (Figure 1a, blue line) (Wang, Mizaikoff, & Kranz, 2009). It has previously been reported that selecting the spectral region of 1030 to 1400 $cm^{-1}$ improves the sensitivity for the glucose prediction model (Parachalil et al., 2019). However, our previous study shows that only the 1125 $cm^{-1}$ band is sensitive enough for pathophysiologically relevant low glucose level detection and other peaks are highly disrupted below 5 mmol/l. Thus we concluded that univariate data analysis can preferred over multivariate analysis (Golparvar et al., 2021). The glucose Raman shift peak of 1125 $cm^{-1}$ has been assigned to C-O-H bonds' bending mode or C-O-C bonds' antisymmetric stretching mode (Dudek et al.,
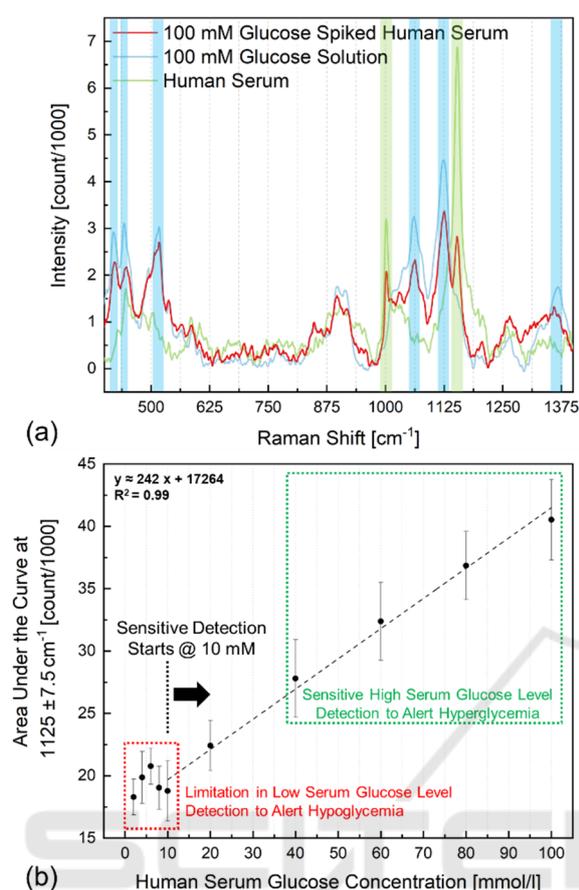
Figure 1: (a) Processed (i.e., background subtracted and smoothed) 532 nm green laser-induced Raman scattering spectra of spiked human serum with 100 mmol/l glucose (red line), human serum without glucose spike (green line), and 100 mmol/l glucose aqueous solution (blue line). The Raman spectrum of the mixture (serum + glucose) consists of the superposition of the individual spectrum of each solution (red line). Laser power and acquisition time were adjusted to 200 mW and 1 minute, respectively. Characteristic peaks of glucose (blue bands) and serum (green bands) are highlighted. (b) The calibration curve for glucose concentration prediction is computed by the area under the curve at $1125 \pm 7.5$ cm$^{-1}$; three consecutive measurements return the standard deviation error bars.

2019; Fujihara, Nishimoto, Yasuda, & Takeshita, 2019). Although our previous study is based on measurement acquired only on water-based solutions (not human serum), it is imperative to address the issue of measuring low concentrations in serum successfully. On the other hand, when induced by a 785 nm near-infrared laser, the strongest serum Raman bands in the fingerprint region appear around 820, 1044, 1335, 1383, 1442, and 1542 cm$^{-1}$, and they are widely associated with CH2 and CH3 groups (i.e., lipids and proteins) (Huang et al., 2011).

However, when human serum is excited by a 532 nm green laser, the Raman peaks of α- and β-carotenes, which in total their concentration is only a few hundred nmol/l in blood serum, resonate and dominate the spectrum (Figure 1a, green line) (Bohn, 2018; Medipally et al., 2017).

Typically, if the laser excitation frequency is close to the frequency of the electronic transition of a molecule, resonance Raman occurs and enhances the otherwise spontaneous Raman effect (Schmitt & Popp, 2006). This well-known phenomenon is traditionally used to study molecules in extremely low concentrations (X. Zhou et al., 2019). Carotenoids' electronic absorption band is anticipated to be between 400 nm and 550 nm, and thus, 532 nm laser energy lies close enough to its electronic transition to trigger the resonance Raman effect (Fran Adar, 2017). However, in serum glucose detection, this is an unwanted enhancement and the very stable 1153 cm$^{-1}$ resonant Raman band of total carotenoids interferes with the targeted glucose 1125 cm$^{-1}$ band. Although for univariate analysis of high glucose levels (10–100 mmol/l), this is not an issue, and the calibration curve is linearly fit with an $R^2$ value of 0.99 and sensitivity of $\sim$ 242 counts/mM, in lower glucose levels (1–8 mmol/l), the detection is limited. In high glucose concentrations, the 1125 cm$^{-1}$ peak is strong and distinguishable as same as the 1153 cm$^{-1}$ peak (Figure 1a, red line), but when the intensity of glucose 1125 cm$^{-1}$ peak decreases due to the decrease in concentration, it becomes a shoulder peak to the 1153 cm$^{-1}$ and completely vanishes below $\sim$ 8 mmol/l. As a result, the measurement should go through specific optimizations to detect low serum glucose levels with 532 nm green laser-induced spontaneous Raman spectroscopy.

The optimal focus depth of the laser beam in the solutions affects the number of received inelastically scattered photons and can be tuned to increase detection sensitivity (Dubessy, Lhomme, Boiron, & Rull, 2002). This is validated using four focus depths while concentration, laser power, and acquisition time were kept constant (Figure 2a). Furthermore, different droplets of the same solution were used each time to ensure the intensity difference between measurements is not induced by heat changes in the region of focus due to the laser power. By fine-tuning the z-axis of the objective stage, the focus depth changed. Figure 2a illustrates that the laser beam yields the lowest Raman intensity when focused on the aqueous glucose solution's surface (depth = 0 um). Instead, the intensity slightly decreases with the focus depth below the solution's surface (e.g., more scattering at a depth of 200 um compared to 400 um).
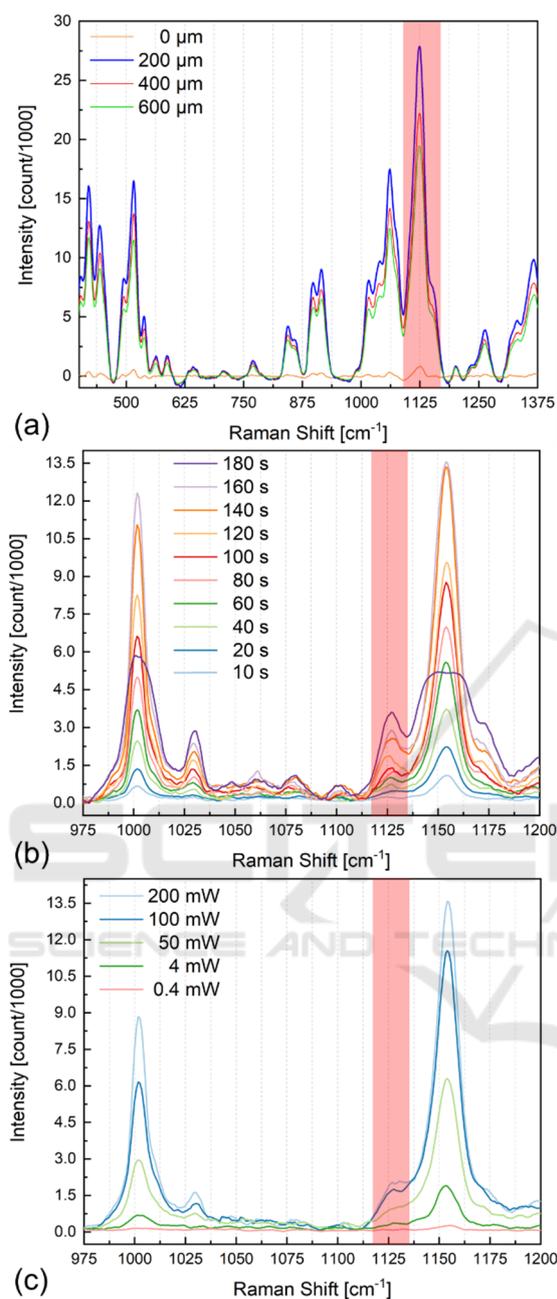
(a)

(b)

(c)

Figure 2: Optimizations for univariate detection of low glucose concentration using merely 1125 cm^{-1} band from human serum with 532 nm green laser-induced Raman spectroscopy in interference with carotenoids' resonance Raman band of 1153 cm^{-1}. Intensity dependency of 1125 cm^{-1} band to (a) depth of focus variation, (b) acquisition time, and (c) laser power variation.

On the other hand, increasing the laser power and the acquisition time increases the sensitivity of Raman spectra (Braun et al., 2016). Figure 2b illustrates the processed Raman spectra of 5 mmol/l
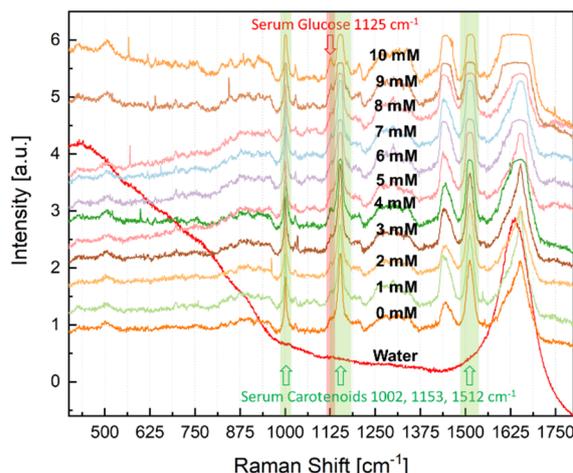


Figure 3: Unprocessed Raman scattering spectra of 532 nm green laser-induced human serum with glucose concentrations ranging from 10 mmol/l to severe hypoglycemic ranges and nanopure water. The depth of laser focus is 200 μm inside the solution droplet, the excitation duration is 3 minutes, and the laser power is 400 mW. The highlighted characteristic Raman peak of glucose 1125 cm^{-1} appears as a small shoulder to the strong carotenoid resonance peak of 1153 cm^{-1} but is still distinguishable due to the applied optimizations. Offsets are added for clarity.

glucose spiked serum with 400 mW of power with different acquisition times varied from 10 s to 180 s in the signature region. Data show that the signal by glucose at 1125 cm^{-1} stays stable, although the strong total carotenoid resonance peaks saturate in the acquisition time of 180 s. Figure 2c illustrates the processed Raman spectra for the same samples but with an acquisition time of 120 s and different laser power varied from 0.4 mW to 200 mW. Figure 2c shows that the 200 mW is not enough to detect low glucose levels in serum because of the interference with the total carotenoids resonance band.

Figure 3. illustrates the unprocessed serum Raman spectra with glucose concentrations ranging from 0 mmol/l to 10 mmol/l obtained by considering all the discussed optimization (depth of laser focus 200 μm, excitation duration 3 minutes, and laser power 400 mW). The highlighted glucose Raman shift peak is stable and can be used in the univariate analysis, calculating merely the area under the curve at 1125 ± 7.5 cm^{-1}, even though the 1153 cm^{-1} and 1512 cm^{-1} resonance carotenoid pecks saturated already at 4 mmol/l of glucose in the serum.

Figure 4a. illustrates the filtered spectra from Figure 3 in the region of interest, as highlighted, and Figure 4b shows the obtained calibration curve by recording an excellent linear fit (randomly scattered

data in the residual plot was recorded) with $R^2$ value of 0.98, the sensitivity of $\sim$ 2606 counts/mM, and root mean square of the error or residual standard deviation of 0.6. The theoretical limit of detection (LOD) is calculated with (1) in accordance with recommendations by the International Union of Pure and Applied Chemistry (IUPAC) definitions (Stacey, Mader, & Sammon, 2017; Vandenabeele & Moens, 2012).

$$LOD = K\delta/S \approx 1.2 \text{ mmol/l} \qquad (1)$$

Where K is the confidence coefficient (usually K=3 with a confidence level of 99.86%), $\delta$ is the standard deviation of the blank measurement (here $\sim$ 1066.9 counts), and S is the slope of the calibration curve (here $\sim$ 2606 counts/mM).
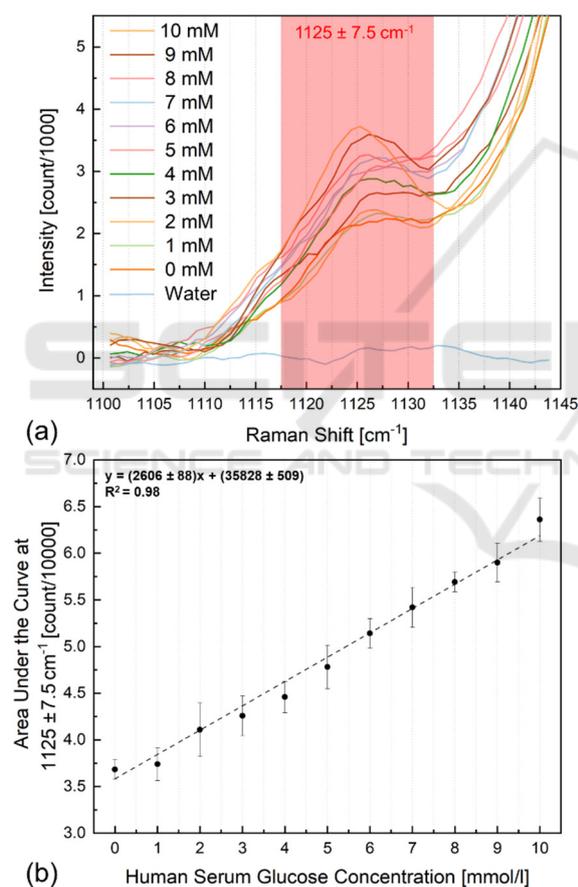


Figure 4: (a) Processed Raman scattering spectra of human serum with glucose concentrations below 10 mmol/l and water; the characteristic peak under analysis is highlighted. The visual evaluation of the Raman shift around 1125 cm$^{-1}$ indicates the glucose level increase as a function of its concentration. (b) The calibration curve for glucose concentration prediction is computed by the area under the curve at $1125 \pm 7.5$ cm$^{-1}$; three consecutive measurements return the standard deviation error bars. Sensitivity $\approx$ 2606 counts/mM and LOD $\approx$ 1.2 mmol/l.

# 4 CONCLUSION

The 532 nm green laser-induced autofluorescence appears as background noise in the human serum Raman spectra but can be filtered out. Therefore, it is feasible to acquire 532 nm excitation source for glucose detection, while it appears highly advantageous to improve the efficiency of the Raman scattering (up to almost 16 times) with respect to near-infrared wavelengths. Furthermore, 532 nm laser choice is optimal for low-cost applications with CMOS imagers. In fact, their highest quantum efficiency (QE) at this wavelength is increased by a further 37.5%: i.e., typically CMOS imagers QE at 532 nm is $\sim$ 95% while is only 65% at 785 nm). Of course, total carotenoids resonance appears when 532 nm laser is utilized in spontaneous Raman spectroscopy on full human serum. Although this is not an issue for high glucose concentrations (e.g., in the case of hyperglycemia monitoring), this resonance by carotenoids limits the detection of lower glucose levels (below 10 mmol/l, or 180 mg/dl). These levels are of top importance to monitor because they typically correspond to those of hypoglycemic patients, indeed.

Therefore, this study investigated possible optimizations on laser focal depth, laser excitation duration, and laser power to extend the sensitivity of the measurement to low glucose ranges in order to open the monitoring of hypoglycemic ranges below 2.2 mmol/l (40 mg/dl), usually neglected in applications of Raman detection of glucose for the limitations we have described in this paper. Indeed, the calibration curve we have recorded on serum samples by applying the mentioned optimized tuned parameters was enough sensitive and linear in the range of 0–10 mmol/l, with a limit of detection (LOD) at 1.2 mmol/l only. Therefore, this study confirms that Raman spectroscopy is useful to measure endogenous compounds in lower concentrations also in the case their peak are typically present close to the region of Raman shift where carotenoid-interference is usually present.

Future developments will be focused to directly detect urea and lactate in lower concentration ranges as well, in human serum, with 532 nm-induced Raman spectroscopy, by merely analyzing their single Raman signatures bands. Lactate has a characteristic peak around 861 cm$^{-1}$, and urea has a strong characteristic presence around 1005 cm$^{-1}$ (Golparvar et al., 2021). Although lactate characteristic peak hypothetically will not interfere with any of the carotenoids resonance bands, urea's characteristic peak will interfere with the resonance

band of total carotenoids at 1002 cm$^{-1}$, and further investigations should be carried out similarly to optimize the selectivity for urea.

## ACKNOWLEDGMENTS

## REFERENCES

Abdoli, S., Hessler, D., Vora, A., Smither, B., & Stuckey, H. (2020). Descriptions of diabetes burnout from individuals with Type 1 diabetes: an analysis of YouTube videos. *Diabetic Medicine, 37*(8), 1344-1351.

Adar, F. (2017). Carotenoids-their resonance Raman spectra and how they can be helpful in characterizing a number of biological systems. *Spectroscopy, 32*(6), 12-20.

Adar, F., Lee, E., Mamedov, S., & Whitley, A. (2010). Experimental evaluation of the depth resolution of a Raman microscope. *Microscopy and Microanalysis, 16*(S2), 360-361.

Asharani, P., Wu, Y. L., Gong, Z., & Valiyaveettil, S. (2008). Toxicity of silver nanoparticles in zebrafish models. *Nanotechnology, 19*(25), 255102.

Bohn, T. (2018). Metabolic fate of bioaccessible and non-bioaccessible carotenoids. *Non-Extractable Polyphenols and Carotenoids: Importance in Human Nutrition and Health*, 165-200.

Bommer, C., Sagalova, V., Heesemann, E., Manne-Goehler, J., Atun, R., Bärnighausen, T., . . . Vollmer, S. (2018). Global economic burden of diabetes in adults: projections from 2015 to 2030. *Diabetes care, 41*(5), 963-970.

Boukhayma, A. (2018). Low-noise CMOS image sensors. In *Ultra Low Noise CMOS Image Sensors* (pp. 13-34): Springer.

Boukhayma, A., Peizerat, A., & Enz, C. (2016). A sub-0.5 electron read noise VGA image sensor in a standard CMOS process. *IEEE Journal of solid-state circuits, 51*(9), 2180-2191.

Braun, F., Schwolow, S., Seltenreich, J., Kockmann, N., Röder, T., Gretz, N., & Rädle, M. (2016). Highly sensitive Raman spectroscopy with low laser power for fast in-line reaction and multiphase flow monitoring. *Analytical chemistry, 88*(19), 9368-9374.

Brinati, L. M., de Fátima Januário, C., Balbino, P. C., Gonçalves Rezende Macieira, T., Cardoso, S. A., Moreira, T. R., & de Oliveira Salgado, P. (2021). Incidence and Prediction of Unstable Blood Glucose Level among Critically Ill Patients: A Cohort Study. *International Journal of Nursing Knowledge, 32*(2), 96-102.

Chege, B. M., Birech, Z., Mwangi, P. W., & Bukachi, F. O. (2019). Utility of Raman spectroscopy in diabetes detection based on biomarker Raman bands and in antidiabetic efficacy studies of herbal extract Rotheca myricoides Hochst. *Journal of Raman Spectroscopy, 50*(10), 1358-1366.

Dubessy, J., Lhomme, T., Boiron, M.-C., & Rull, F. (2002). Determination of chlorinity in aqueous fluids using Raman spectroscopy of the stretching band of water at room temperature: application to fluid inclusions. *Applied spectroscopy*, 56(1), 99-106.

Dudek, M., Zajac, G., Szafraniec, E., Wiercigroch, E., Tott, S., Malek, K., . . . Baranska, M. (2019). Raman Optical Activity and Raman spectroscopy of carbohydrates in solution. *Spectrochimica Acta Part A: Molecular and Biomolecular Spectroscopy, 206*, 597-612.

Fujihara, J., Nishimoto, N., Yasuda, T., & Takeshita, H. (2019). Discrimination between infant and adult bloodstains using micro-Raman spectroscopy: A preliminary study. *Journal of forensic sciences, 64*(3), 698-701.

Golparvar, A., Boukhayma, A., Loayza, T., Caizzone, A., Enz, C., & Carrara, S. (2021). Very Selective Detection of Low Physiopathological Glucose Levels by Spontaneous Raman Spectroscopy with Univariate Data Analysis. *BioNanoScience*, 1-7.

Greer, J. S., Petrov, G. I., & Yakovlev, V. V. (2013). Raman spectroscopy with LED excitation source. *Journal of Raman Spectroscopy, 44*(7), 1058-1059.

Gulyamov, S., Shamshiddinova, M., Bae, W. H., Park, Y. C., Kim, H. J., Cho, W. B., & Lee, Y. M. (2021). Identification of biomarkers on kidney failure by Raman spectroscopy. *Journal of Raman Spectroscopy*.

Huang, N., Short, M., Zhao, J., Wang, H., Lui, H., Korbelik, M., & Zeng, H. (2011). Full range characterization of the Raman spectra of organs in a murine model. *Optics express, 19*(23), 22892-22909.

Ju, J., Hsieh, C.-M., Tian, Y., Kang, J., Chia, R., Chang, H., . . . Liu, Q. (2020). Surface enhanced Raman spectroscopy based biosensor with a microneedle array for minimally invasive in vivo glucose measurements. *ACS sensors, 5*(6), 1777-1785.

Kang, J. W., Park, Y. S., Chang, H., Lee, W., Singh, S. P., Choi, W., . . . Park, J. (2020). Direct observation of glucose fingerprint using in vivo Raman spectroscopy. *Science Advances, 6*(4), eaay5206.

Kiefer, W. (2007). Recent advances in linear and non-linear Raman spectroscopy I. *Journal of Raman Spectroscopy: An International Journal for Original Work in all Aspects of Raman Spectroscopy, Including Higher Order Processes, and also Brillouin and Rayleigh Scattering, 38*(12), 1538-1553.

Krishnan, R., & Shankar, R. (1981). Raman effect: History of the discovery. *Journal of Raman Spectroscopy, 10*(1), 1-8.

Lawson, E., Barry, B., Williams, A., & Edwards, H. (1997). Biomedical applications of Raman spectroscopy. *Journal of Raman Spectroscopy, 28*(2-3), 111-117.

Li, Z., Deen, M. J., Kumar, S., & Selvaganapathy, P. R. (2014). Raman spectroscopy for in-line water quality

monitoring—Instrumentation and potential. *Sensors, 14*(9), 17275-17303.

Medipally, D. K., Maguire, A., Bryant, J., Armstrong, J., Dunne, M., Finn, M., . . . Meade, A. D. (2017). Development of a high throughput (HT) Raman spectroscopy method for rapid screening of liquid blood plasma from prostate cancer patients. *Analyst, 142*(8), 1216-1226.

Mhlanga, N., Tetyana, P., Nyembe, S., & Sikhwivhilu, L. (2021). Application of Raman Spectroscopy in Biomedical Diagnostics. In *Recent Developments in Atomic Force Microscopy and Raman Spectroscopy for Materials Characterization*: IntechOpen.

Parachalil, D. R., Bruno, C., Bonnier, F., Blasco, H., Chourpa, I., McIntyre, J., & Byrne, H. J. (2019). Raman spectroscopic screening of high and low molecular weight fractions of human serum. *Analyst, 144*(14), 4295-4311.

Schmitt, M., & Popp, J. (2006). Raman spectroscopy at the beginning of the twenty-first century. *Journal of Raman Spectroscopy: An International Journal for Original Work in all Aspects of Raman Spectroscopy, Including Higher Order Processes, and also Brillouin and Rayleigh Scattering, 37*(1-3), 20-28.

Singh, G. P., Goh, S., Canzoneri, M., & Ram, R. J. (2015). Raman spectroscopy of complex defined media: biopharmaceutical applications. *Journal of Raman Spectroscopy, 46*(6), 545-550.

Smith, J. L. (2015). The pursuit of non-invasive glucose: hunting the deceitful turkey. *Revised and Expanded, copyright*.

Stacey, P., Mader, K. T., & Sammon, C. (2017). Feasibility of the quantification of respirable crystalline silica by mass on aerosol sampling filters using Raman microscopy. *Journal of Raman Spectroscopy, 48*(5), 720-725.

Stuart, D. A., Yuen, J. M., Shah, N., Lyandres, O., Yonzon, C. R., Glucksberg, M. R., . . . Van Duyne, R. P. (2006). In vivo glucose measurement by surface-enhanced Raman spectroscopy. *Analytical chemistry, 78*(20), 7211-7215.

Šugar, J., & Bouř, P. (2016). Quantitative analysis of sugar composition in honey using 532-nm excitation Raman and Raman optical activity spectra. *Journal of Raman Spectroscopy, 47*(11), 1298-1303.

Tuschel, D. (2020). Spectral Resolution and Dispersion in Raman Spectroscopy. *Spectroscopy, 35*, 9.

Vandenabeele, P., & Moens, L. (2012). Some ideas on the definition of Raman spectroscopic detection limits for the analysis of art and archaeological objects. *Journal of Raman Spectroscopy, 43*(11), 1545-1550.

Wang, L., Mizaikoff, B., & Kranz, C. (2009). Quantification of sugar mixtures with near-infrared Raman spectroscopy and multivariate data analysis. A quantitative analysis laboratory experiment. *Journal of chemical education, 86*(11), 1322.

Wróbel, M. (2016). *Non-invasive blood glucose monitoring with Raman spectroscopy: prospects for device miniaturization.* Paper presented at the IOP Conference Series: Materials Science and Engineering.

Zhou, B., Lu, Y., Hajifathalian, K., Bentham, J., Di Cesare, M., Danaei, G., . . . Taddei, C. (2016). Worldwide trends in diabetes since 1980: a pooled analysis of 751 population-based studies with 4· 4 million participants. *The lancet, 387*(10027), 1513-1530.

Zhou, X., Qin, M., Zhu, J., Wang, C., Zhu, G., Wang, H., & Yang, L. (2019). Rapid and sensitive surface-enhanced resonance Raman spectroscopy detection for norepinephrine in biofluids. *Journal of Raman Spectroscopy, 50*(3), 314-321.

Zimmet, P., Alberti, K., & Shaw, J. (2001). Global and societal implications of the diabetes epidemic. *Nature*, 414(6865), 782-787.